Joint Modeling of the Thermo-Tectonic Evolution in an Extensional Area*

Eugenio Carminati[1], Marco Cuffaro[2], Edie Miglio[3], Carlo Doglioni[1], and Paolo Ruffo[4]

[1]Dipartimento di Scienze della Terra, Sapienza Università di Roma, Italy (eugenio.carminati@uniroma1.it)
[2]IGAG, CNR, Rome, Italy
[3]MOX-Dipartimento di Matematica, Politecnico di Milano, Milan, Italy
[4]ENI E&P, San Donato Milanese, Italy

Abstract

Geometry, sedimentary facies distribution and thermal evolution of extensional basins are controlled by a number of factors and processes, acting at local, regional and global scales: amount and rate of thinning; latitude at which the basin develops; pre-rift thickness and heterogeneities of the lithosphere; amount of clastic sediment supply; number, spacing and dècollement depth of normal faults; sediment supply; sediment compaction; plate motions relative to the mantle.

Using a natural example from the Central Southern Alps, we show that, if a reasonable knowledge of the thermal parameters of both covers and basement is available, thermo-kinematic modeling can provide useful first-order estimates in frontier areas of heat flow and temperature evolution through time. The Southern Alps were characterised by strong variations, both in space and time, of heat flow during Mesozoic rifting (Figure 1). The regional thermal history was reconstructed using organic matter (OM) maturity data from outcropping sediments. It is generally agreed that the main extensional phases in the Southern Alps developed from Late Permian to Middle Jurassic (e.g. Doglioni and Carminati, 2008). However, some evidence of extensional activity has been described also for Upper Jurassic-Lower Cretaceous times (Doglioni, 1992a-b), as also suggested by thickness variations in Figure 1a. The stratigraphy shown in Figure 1a, obtained by retro-deforming the shortening associated with the Alpine orogeny, is referred to the Cretaceous and was used as input for thermo-kinematic calculations performed using TECMOD2D software (http://www.geomodsol.com; Grigo and Schmalholz, 2003), as broadly discussed in Carminati et al. (2010).

Modeling Southern Alps Rift Zone

Figure 1b shows the heat flow distribution through time obtained inverting the stratigraphy shown in Figure 1a. Panels 1c and 1d show the delta and beta factors necessary to produce the accommodation space for the sedimentary piles deposited in the Southern Alps rift zone and passive margin. As can be observed, the stretching factors are rather variable through time, being high in the Permian and in the Early Jurassic and rather negligible for Cretaceous time. Figure 2 shows a comparison between the vitrinite reflectance measured by Scotti (2005) at the Iseo W location (Figure 1) and the model predictions. The purpose of this figure is to show how different parameters locally affect the predicted vitrinite reflectance. In Figure 2a, the colored curves refer to models with the optimal set of kinematic and thermal parameters, with heat production of the upper crustal rocks ranging between $2 \cdot 10^{-6}$ and $6 \cdot 10^{-6}$ W/m^3 and with sediment heat production of $1 \cdot 10^{-6}$ W/m^3. The predicted curves match quite well the trend of the measured vitrinite reflectance. However, the magnitude of the R$_o$% is generally underestimated, with smaller errors for the models characterised by highest crustal heat flow production. Figure 2b shows the influence of sediment heat production on the vitrinite reflectance predictions. The misfit at deeper depths is reduced with respect to the models of Figure 2a, but the misfit at shallower depths is left unchanged.

In Figure 2c and Figure 2d, the effects of the post-Aptian siliciclastic sediments on the vitrinite reflectance predictions are shown. From this panel it can be concluded that the inclusion of the post Aptian sediments is necessary to reproduce adequately the measured vitrinite reflectances. These results show that the largest array of available observations should be used to constrain thermo-kinematic models. This may not be possible in frontier areas. Therefore, in such areas the results of thermo-kinematic models should be considered as first order approximations of the real solution.

As briefly shown, the temperature distribution, and consequently the maturity of organic matter in sediments, is strongly dependent on the thermal parameters adopted and on the heat flow coming from the mantle. This latter feature is controlled by plate, or even global scale processes. In resource assessment, global scale processes are normally neglected. With this contribution we aim at filling, at least partially, this gap.

Modeling Mid-Ocean Ridges

Tectonic evolution at rift zones is commonly considered symmetric along mid-ocean ridges (MORs), when dealing with relative plate motions and steady-state processes. The oceanic lithosphere is created at MORs, while the two plates are moving away from each other on both sides of the fixed ridge. When the plates diverge, the hot rocks of the underlying mantle, i.e. the asthenosphere, flow upward beneath the MOR and accrete to the base of the spreading plates, becoming part of them, due to cooling effects by conductive heat loss at the surface. As the plates steadily move away to the oceanic ridge, they continue to be affected by thermal cooling, and the lithosphere thickens. The base of lithosphere is assumed to be approximately coincident with the depth of the T_M=1350° C isotherm,

corresponding to a viscosity $\eta = 10^{19}$ Pa s. A basic step in the geodynamic modeling of MOR evolution corresponds to the choice of plate velocities as boundary conditions. Generally, relative plate motions are used, where plates move with respect to a fixed ridge axis, with a half spreading velocity V_{hsr}. When using these model parameters, mantle flow field is expected to rise under the fixed ridge with a symmetric pattern, and also the accretion of the oceanic lithosphere is predicted to be symmetric.

However, the bathymetry of rift zones is generally asymmetric, being the eastern flank on average slightly shallower (100-300 m) than the western one (Doglioni et al., 2003). Also, based on surface wave tomographic models, shear wave velocities in the upper mantle indicate a difference between the western and eastern flanks of an oceanic basin (Panza et al., 2010).

Moreover, when MOR migration is taken into account in the geodynamic models, plate motions referred to the mantle have to be introduced. Mantle-reference (or absolute) motions describe how the entire lithosphere moves relative to the mantle, and they represent a more appropriate framework for comparisons with results of plate dynamic models. The hotspot framework is a good reference system, where to evaluate absolute plate motions. It is based on the assumption that the hotspots are fixed relative to the deep mantle and to each other (Morgan, 1971; Wilson, 1973), and the orientation and the age progressions along their surface traces reflect the motion of the overlying lithospheric plate relative to the hotspots (e.g., the Hawaiian sea-mount track). Under these assumptions, current global scale plate motions can be computed (Gripp and Gordon, 2002; Cuffaro and Jurdy, 2006). In absolute frameworks, a net "westward" rotation of the lithosphere relative to the mantle can be observed, and we used velocities obtained in the hotspot reference frame, as boundary conditions. This implies that plates along a ridge, and the ridge itself, move toward the west but with different velocities, relative to the fixed mantle, and the separation between plates triggers mantle upwelling.

The mantle can be modeled as a viscous fluid, and its dynamics can be described using the Stokes equations. At a first approximation the fluid is considered Newtonian. A further step in the description of the phenomena would require the inclusion of thermal effects: in this case the fluid viscosity and density have to be considered as a function of the temperature. For solving both the Stokes equations and the thermal effects, a finite element approach has been adopted.

Here, we consider both the models of passive mantle upwelling beneath a MOR, using relative and absolute plate motions, as boundary conditions, for stationary and transient plate tectonic processes respectively, to investigate evolution of the spreading centers, and lithosphere/mantle interaction in the ocean basins. The variable viscosity condition proposed by Shen and Forsyth (1992) is used in these models, and the computations are applied to the Atlantic Ocean, across the Mid-Atlantic Ridge (MAR) representing the boundary between the North America and Eurasia plates, quantifying the conceptual model proposed by Carminati et al. (2009). In these computations, we used plate-driven mantle upwelling assumptions and thermal effects, not including mantle melting and lateral variations of mantle density, so that we choose to model tectonic evolution at MORs as a passive process.

The particular choice of initial and boundary conditions used in the simulation are reported as it follows. In particular, on the bottom of the Cartesian domain, the velocity and the stress are assumed to be normal to the boundary. On the lateral boundaries, a velocity profile normal to the boundary is imposed, depending on the choice of the plate kinematic framework. On the top, the tangential component of the velocity is assigned and the normal component is zero. As for the temperature, on the lateral boundaries a zero thermal flux is imposed, whereas the temperature is assigned on the top and on the bottom of the domain. We also used the half spreading rate V_{hsr}=15 mm/a, obtained by DeMets, Gordon, Argus, and Stein (1994) in the ridge axis reference frame, and V_{NA}=36 mm/a, V_{MAR}=26 mm/a, and V_{EU}=16 mm/a for velocities of North America, Mid-Atlantic ridge (MAR), and Eurasia respectively, obtained by Gripp and Gordon (2002) in the hotspot framework.

Results of 2D numerical simulations show substantial differences when modeling with a steady-state approach or a time-dependent one. Moreover, these differences are also linked to the choice of the kinematic framework, i.e. relative versus mantle-reference plate motions.

Figure 3 refers to the numerical simulations in the Atlantic Ocean, by making use of a steady-state regime for viscosity flow beneath plates that thicken with increasing age. The MAR is assumed to be fixed, and passive mantle velocity field results in a symmetric pattern; as for the temperature a similar symmetric behaviour is obtained. The base of the lithosphere, corresponding to the depth of the line 19.1 of the $\log_{10}(\eta)$, is symmetric as well, with a minimum depth of -70 km on lateral boundaries, and a maximum one of -10 km beneath the ridge axis, in the whole domain of the simulation (400 km).

Significantly different results are obtained when computing evolution of MORs using a time-dependent approach, and mantle-reference velocities as boundary conditions.   In this second case, the MAR migrates relative to the mantle during the opening of the Atlantic Ocean, in the last 10 Ma, and plates move with different velocities. These conditions trigger mantle upwelling beneath the MAR, and the obtained mantle flow field is asymmetric (Figure 4). In order to emphasize the shear between the lithosphere and the astenosphere, the horizontal components of the velocity field have been recalculated such that a null horizontal velocity component is obtained on the base of the lithosphere, i.e., the line 19.1 of the $\log_{10}(\eta)$. This configuration shows that the North-America and Eurasia plates, and the MAR itself, are moving toward the west, whereas the mantle relatively flows toward the east. During the evolution of the last 10 Ma for the Atlantic Ocean, the mantle flow rises upward beneath the migrating spreading center, contributing to an asymmetric accretion of the lithosphere. This asymmetric shape is a direct consequence of the asymmetric pattern of the temperature field. Considering the 200 km domain (vertical dashed lines, Figure 4), representing the final stage of the simulation (0 Ma, the Present), the base of the lithosphere reaches two different depths: approximately -85 km on the western flank (North America) and -75 km on the eastern one (Eurasia), providing a different thickness of the lithosphere at the two sides of the ridge. These results

show an asymmetric thickening of plates along the ridge, as suggested by geological and geophysical observations, and provide useful relationships between mantle temperature and thickness of the oceanic lithosphere.

Conclusions

Although the calculations were built for the Atlantic Ocean, conceptually similar results are expected for rifts and oceanizations that occurred in the past. As a consequence, the fossil passive margins developed to the east and to the west of paleo MOR should be underlined by hotter and colder asthenospheric mantle, respectively. As a consequence, a shallower base of the lithosphere is expected to occur along passive margins to the east of MORs. Shallower base of the lithosphere implies higher heat fluxes from the mantle and potentially steeper temperature profiles in the sedimentary piles deposited along such rift zones and passive margins. Consequently, the temperature distribution, through time, in sediments deposited along conjugate margins could be significantly different. In this contribution we couple, for the first time, the results from 2D thermo-kinematic models and those of 2D plate scale models to evaluate whether such differences could have economic consequences. The coupling is provided by the use of the results of global model as forcing factors in local/regional thermo-kinematic models. Once again, the Southern Alps rifting will be used as a natural laboratory in this respect. In particular, global models show that, beneath passive margins to the east of rift zones, the depth of the lithosphere can be shallower by some 10 km with respect to western passive margins. If such a difference in the depth of the base of the lithosphere is imposed to 2D thermo-kinematic models for the Southern Alps, non-negligible differences in the temperature distribution within the basin are obtained.

Acknowledgements

References

Bertotti, G., V. Picotti, D. Bernoulli, and A. Castellarin, 1993a, From rifting to drifting: tectonic evolution of the Southalpine upper crust from the Triassic to the Early Cretaceous: Sedimentary Geology, v. 86, p. 53-76.

Carminati, E., D. Cavazza, D. Scrocca, R. Fantoni, P. Scotti, C. Doglioni, 2010, Thermal and tectonic evolution of the Southern Alps (Northern Italy) rifting: coupled organic matter maturity analysis and thermo-kinematic modelling, Bulletin of the American Association of Petroleum Geologists, v. 94, p. 369-397.

Carminati, E., M. Cuffaro, and C. Doglioni, 2009, Cenozoic uplift of Europe: Tectonics, v. 28, doi:10.1029/2009TC00247.

Cuffaro, M., and D.M. Jurdy, 2006, Microplate motions in the hotspot reference frame: Terra Nova, v. 18, p. 276-281.

DeMets, C., R.G. Gordon, D.F. Argus, and S. Stein, 1994, Effect of recent revisions to the geomagnetic reversal time scale on estimates of current plate motions: Geophysical Research Letters, v. 21, p. 2121-2194.

Doglioni, C., and E. Carminati, 2008, Structural styles and Dolomites field trip: *Memorie Descrittive della Carta GEologica d'Italia*, v. 82, p. 1-299.

Doglioni, C., E. Carminati, and E. Bonatti, 2003, Rift asymmetry and continental uplift: Tectonics, v. 22, doi:10.1029/2002TC001459.

Doglioni, C., 1992, The Venetian Alps thrust belt, *in* K.R. McClay (Ed.), Thrust Tectonics: Chapman and Hall, London, p. 319-324.

Doglioni, C., 1992b, Relationships between Mesozoic extensional tectonics, stratigraphy and Alpine inversion in the Southern Alps: *Eclogae Geologicae Helvetiae*, v. 85, p. 105-126.

Fantoni, R., and P. Scotti, 2003, Thermal record of the Mesozoic extensional tectonics in the Southern Alps: *Atti Ticensi Scienze della Terra*, SS9, p. 96-101.
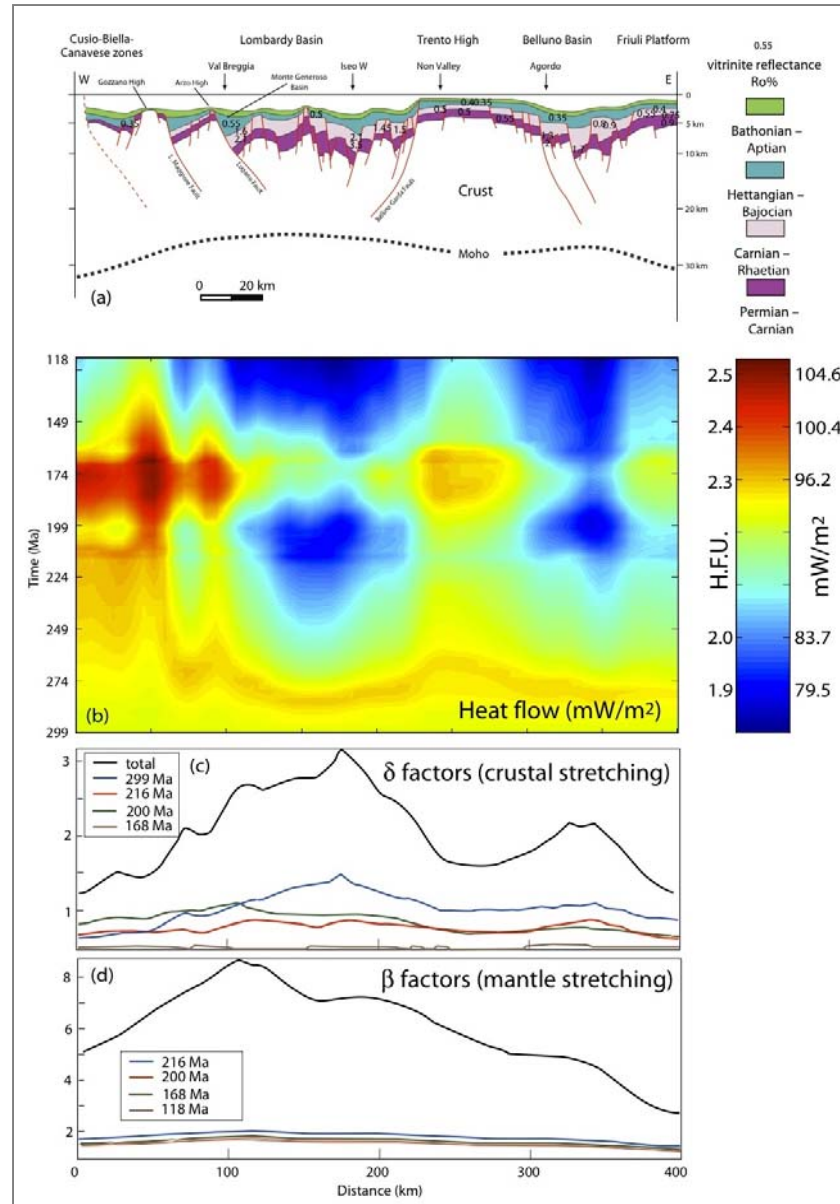
Figure 1. (a) Extensional Mesozoic architecture of the Southern Alps at the end of Lower Cretaceous time (modified after Bertotti et al., 1993 in Fantoni and Scotti, 2003). Organic matter maturity (vitrinite reflectance – R_o %) after Fantoni and Scotti (2003). The Upper Cretaceous crustal structure is only speculative and does not reflect the present day crustal thicknesses, which have been increased by Alpine compressional tectonics. (b) Heat flow distribution through time at the top of the basement obtained assuming, for the upper crust, a radiogenic heat production of $4 \cdot 10^{-6}$ W/m^3. (c) and (d) crustal stretching and mantle stretching factors respectively. All the panes are taken from Carminati et al., 2010.
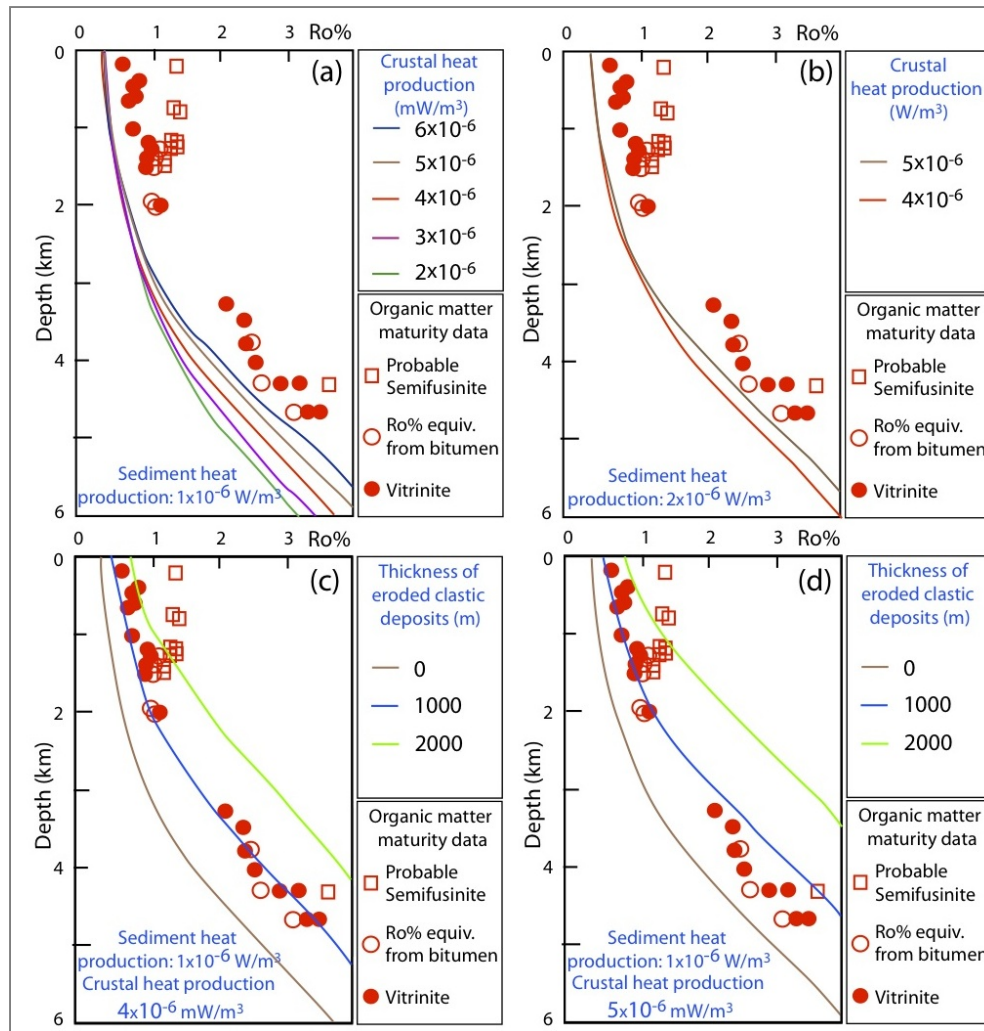
Figure 2. Along depth comparison between the vitrinite reflectance measured by Fantoni and Scotti (2003) at the Iseo W location (Figure 1a) and model predictions. a) The various coloured curves are referred to models with the optimal set of kinematic and thermal parameters, with heat production of the upper crustal rocks ranging between $2 \cdot 10^{-6}$ and $6 \cdot 10^{-6}$ W/m^3 and with sediment heat production of $1 \cdot 10^{-6}$ W/m^3. b) The colored curves refer to models with the optimal set of kinematic and thermal parameters, with heat production of the upper crustal rocks ranging between $4 \cdot 10^{-6}$ and $5 \cdot 10^{-6}$ W/m^3 and with sediment heat production of $2 \cdot 10^{-6}$ W/m^3. c) The curves show the results of models with the optimal set of kinematic and thermal parameters, with heat production of the upper crustal rocks of $4 \cdot 10^{-6}$ and with sediment heat production of $1 \cdot 10^{-6}$ W/m^3 varying the thickness of post-Aptian sediments between 0 and 2000 m. d) The curves show the results of models with the optimal set of kinematic and thermal parameters, with heat production of the upper crustal rocks of $5 \cdot 10^{-6}$ W/m^3 and with sediment heat production of $1 \cdot 10^{-6}$ W/m^3 varying the thickness of post-Aptian sediments between 0 and 2000 m. After Carminati et al., 2010.
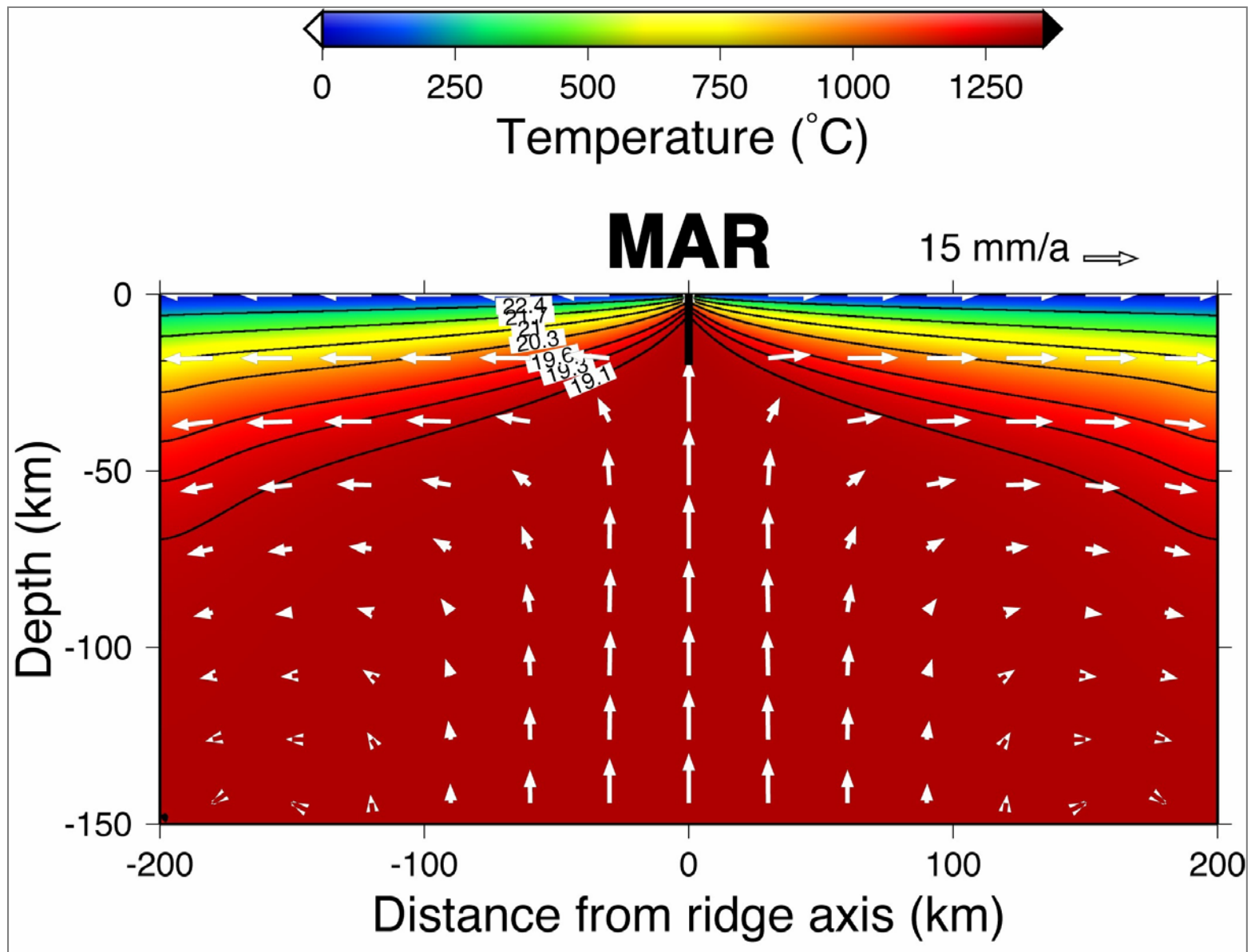
Figure 3. Results of numerical simulations in a steady-state regime for viscosity flow beneath plates that thicken with increasing age. The Mid-Atlantic ridge (MAR) is fixed and passive mantle velocity field (white arrows) is symmetric. Colors are related to the distribution of the temperature. Contour lines represent the Log of the temperature dependent viscosity. The transition between the lithosphere and asthenosphere is assumed to correspond in our calculations to the depth of the line 19.1, that results in a symmetric shape.
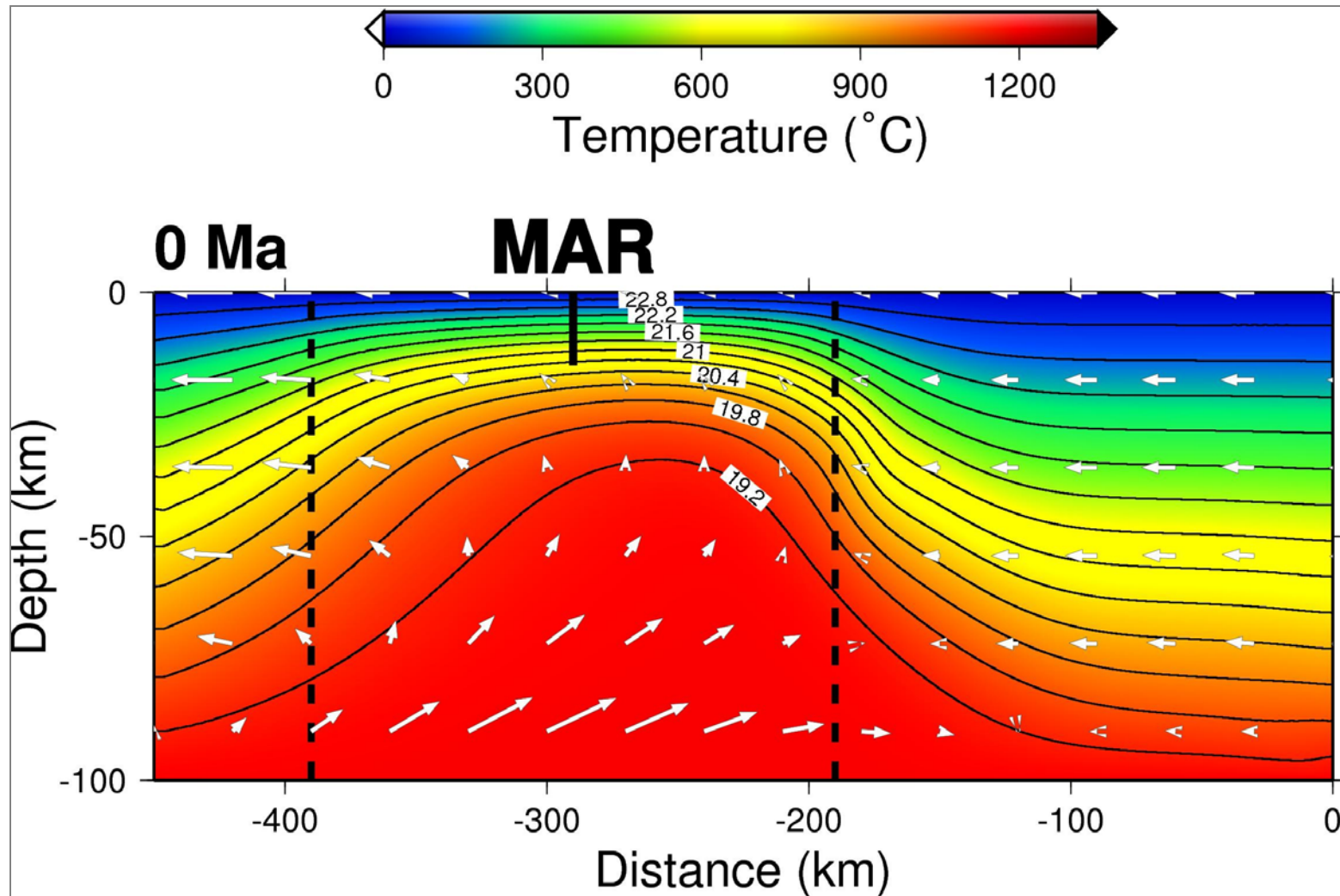
Figure 4. Results of numerical simulations in a time-dependent regime for viscosity flow beneath plates that thicken with increasing age, for the final step of the evolution, the Present (0 Ma). Colors are related to the distribution of the temperature, and contour lines represent the Log of the temperature dependent viscosity. The transition between the lithosphere and asthenosphere is assumed to correspond to the depth of the 19.1, that results in an asymmetric shape, and passive mantle velocity field scaled on the contour line 19.1 (white arrows) is asymmetric. Vertical dashed lines represent the opening of the Atlantic Ocean during the last 10 Ma.